Estimation of Moving Vehicle Locations Using Wheel Shape Information in Single 2-D Lateral Vehicle Images by 3-D Computer Vision Techniques

Chih-Chiun Lai (賴志群) and Wen-Hsiang Tsai (蔡文祥)

Department of Computer and Information Science
National Chiao Tung University, Hsinchu, Taiwan 300, Republic of China
Tel: (03)5712121 Ext. 56650 Fax: (03)5721490 E-mail: gis82805@cis.nctu.edu.tw

ABSTRACT

An approach to the estimation of moving lateral vehicle locations for driving assistance using wheel shape information in single 2-D vehicle images by 3-D computer vision techniques is proposed. The location scheme is supposed to be performed on a vehicle with a camera mounted on the front bumper. The rear wheel shape of a lateral vehicle moving in a nearby lane is imaged in sequence. At first, by using the Hough transform, the projected wheel shape, which is an ellipse, is detected. An edge point verification algorithm is utilized to extract the ellipse shape more precisely. The equation of the ellipse is then computed and used to infer an analytical solution of the orientation angle of the lateral vehicle with respect to the camera view direction. Finally, the center of the ellipse shape is computed and used to determine the relative position of the lateral vehicle with respect to the camera lens center. Both computer-simulated and real images are tested and good experimental results show the effectiveness of the proposed approach for estimating lateral vehicle locations.

Keywords : estimation of lateral vehicle location, driving assistance, wheel shape, ellipse detection, computer vision

1. Introduction

An important application of autonomous vehicle researches by computer vision techniques is human driving assistance. In a traffic environment, there are three views that a driver should take care: the front view, the rear view and the lateral views. Most researches [1-3,6,7] so far focus on vehicle or obstacle detection in the front view for collision avoidance, and on road or line following methods for vehicle guidance. There are some studies [4,5] about observing the vehicle rear view. On the other hand, when driving a vehicle in a certain lane on a road, a driver should notice whether there exists a vehicle in a nearby lane. This is necessary when the driver wants to drive into the nearby lane, or when a vehicle in a nearby lane is trying to get into the driver's lane. There are still very few studies on the detection and location of the lateral vehicle under such circumstances. In this study, the wheel shape information of the lateral vehicle is employed to locate the lateral vehicle, in which the wheel information is captured with a camera mounted on the driver's vehicle. The proposed approach is based on computer vision techniques.

In recent years, a lot of related studies about vehicle detection and location have been proposed [1-7]. For model-based location of vehicles, Ku and Tsai [1] and Lee et al. [2] both used a pre-learned model. By matching the image and the model information, the location of a vehicle is obtained, which is used for vehicle guidance. However, these approaches cannot be utilized to get the location of a lateral vehicle according to the information acquired with the camera.

For vehicle detection and tracking in the front, Charkari and Mori [3] proposed a method to detect a moving vehicle in front of a robot from the forward direction. The intensity value of the vehicle's underneath is used to detect the vehicle boundary, and a dynamic tracking window is used to track the moving vehicle. Then the velocity of the vehicle is determined by the time interval of two consecutive image processing stages. Sasaki at el. [4], and Yanaguchi and Nakajima [5] proposed rear-view observing systems using CCD cameras and a ultrasonic sensors, respectively. However, these approaches[3-5] are not suitable for handling lateral views.

For vehicle trajectory supervision, Chapuis et al.[6] developed a system for the real-time control of the vehicle trajectory on a highway based on an on-board vision system using a single camera. The system has been designed to avoid damages (e.g., due to a sleepy driver). The method is based on the real-time extraction of the relative vehicle location with respect to the lateral road line, and the extracted vehicle location is used to determine the vehicle trajectory. By combining the vehicle trajectory information and some predefined danger criteria, a trajectory supervision module is used to warn the driver when an emergency situation is encountered. In Pomerleau and Jochem[7], an automated vehicle steering system was proposed, which decomposes vehicle steering into three steps: sampling the image, determining the road curvature, and assessing the lateral offset of the vehicle relative to the lane center. As road-departure warning, the system can also compare the assessed lateral offset relative to the lane center with the human driver's steering direction to warn the driver at dangerous time.

All the above systems do not consider lateral vehicle information. When an autonomous vehicle

changes the lane to a nearby one, possible collision with a vehicle on the nearby lane should be avoided. Hence, the extraction of lateral vehicle information is emphasized in this study. A camera is mounted on the right side of the front bumper of the autonomous vehicle and the optical axis of the camera is directed to the lateral side in a certain angle. An illustration of camera setup on a vehicle is shown in Figure 1. A typical view captured by the camera is shown in Figure 2.

To estimate the lateral vehicle location, an image of the vehicle is taken first. This is the start of an image processing stage. The generalized Hough transform[8] is then applied to detect the projected shape of a wheel, which is an ellipse. Because the detected ellipse of the Hough transform may not be the exact projected shape of the wheel but a rough one, an edge point verification procedure is used to compute the ellipse shape more precisely. After the polynomial coefficients of the ellipse equation are determined, the lateral vehicle orientation angle can be obtained by substituting the coefficients into a formula derived in this study. Finally, the center of the ellipse shape is computed and used to determine the relative position of the lateral vehicle with respect to the camera lens center by the backprojection principle. In this study, the projected shape of a wheel is an ellipse with a little rotation, and it is assumed that the ellipse is without rotation. In addition, the heights of the centers of the wheels of the cars of different brands vary within a small range, and it is assumed to be fixed. Hence, some simulations are performed to test whether these assumptions yield tolerant errors.

The major contribution of this study is that the wheel shape information of the lateral vehicle is utilized for the first time. By the estimation of the vehicle location, a lot of useful information is gathered and used for vehicle avoidance, vehicle following, lateral vehicle motion estimation. These applications are useful for autonomous vehicle guidance in the a circumstance with multiple moving vehicles in multiple lanes.

The remainder of this paper is organized as follows. In Section 2, the proposed analytical method to estimate the location of a circle is described. In Section 3, the image processing techniques used to detect an ellipse shape are presented. In Section 4, some experimental results are described. Finally, conclusions and some suggested future works are given in Section 5.

2. Estimation of 3-D Location of a Circular Wheel Shape

In this section, the formulation of the problem of 3-D location of a circular wheel shape and its solution is described. First, we know that the surface normal vector of a wheel of a lateral vehicle is always parallel to the ground plane. Next, we calibrate the camera mounted on the autonomous vehicle in advance in such a way that the swing and tilt angles of the camera with respect to the ground plane are zero. Then, the orientation parameters used to describe the surface normal of a wheel shape can be simplified from three parameters down to one parameter, i.e., the pan angle θ. Hence, the lateral vehicle location with respect to the camera coordinate system can be described with four parameters, one parameter θ for the orientation and three parameters (X_c, Y_c, Z_c) for the position vector of the center of the wheel surface. The geometrical situation is shown in Figure 3. The 3-D location problem is solved in two steps in this study. In the first step, the 3-D orientation parameter of the wheel which is a circle in shape is derived. Second, the 3-D position parameters are derived based on the backprojection principle with the knowledge of the height of the wheel center.

Figure 3 shows the camera coordinate system (CCS), denoted as X-Y-Z, and the image plane $Z=f$, where f is the focus length of the camera. The Z-axis is along the optical axis of the camera. The object coordinate system (OCS), denoted as x-y-z, is set up on the wheel of the lateral vehicle, and the z-axis is along the normal vector of the wheel circle through the circle center. The X-Z plane and the x-z plane are both parallel to the ground. The center of the circle O is chosen as the origin of the OCS, and its 3-D coordinates with respect to the CCS are (X_c, Y_c, Z_c). The image coordinate system (ICS) is denoted as u-v. The transformation from the OCS to the CCS [9] can be written as

$$\begin{pmatrix} X \\ Y \\ Z \\ 1 \end{pmatrix} = \begin{bmatrix} \cos\theta & 0 & -\sin\theta & 0 \\ 0 & 1 & 0 & 0 \\ \sin\theta & 0 & \cos\theta & 0 \\ 0 & 0 & 0 & 1 \end{bmatrix} \begin{bmatrix} 1 & 0 & 0 & -X_c \\ 0 & 1 & 0 & -Y_c \\ 0 & 0 & 1 & -Z_c \\ 0 & 0 & 0 & 1 \end{bmatrix} \begin{pmatrix} x \\ y \\ z \\ 1 \end{pmatrix}. \quad (1)$$

Let (u,v) be the coordinates of the perspective projection of a 3-D point (X,Y,Z) on the image plane. The perspective transformation from the OCS(X-Y-Z) to the ICS(u-v) can be written as

$$\begin{pmatrix} u \\ v \end{pmatrix} = \frac{f}{Z} \begin{pmatrix} X \\ Y \end{pmatrix} \quad (2)$$

In addition, the projection of a circle in the image plane is an ellipse and the ellipse equation, which is assumed to have been obtained by some image processing techniques described later, can be expressed as

$$Au^2 + Buv + Cv^2 + Du + Ev + F = 0. \quad (3)$$

The circle equation in the 3-D OCS is expressed as

$$\begin{aligned} x^2 + y^2 &= R^2; \\ z &= 0. \end{aligned} \quad (4)$$

By combining Eq. (1) through Eq. (4), the orientation parameter θ can be obtained. The details are as follows.

First, substitute the expressions of u and v of Eq. (2) into the ellipse equation Eq. (3) to get

$$A\left(\frac{f \cdot X}{Z}\right)^2 + B\left(\frac{f \cdot X}{Z}\right)\left(\frac{f \cdot Y}{Z}\right) + C\left(\frac{f \cdot Y}{Z}\right)^2 + D\left(\frac{f \cdot X}{Z}\right) + E\left(\frac{f \cdot Y}{Z}\right) + F = 0$$

or equivalently,

$$Af^2X^2 + Bf^2XY + Cf^2Y^2 + DfXZ + EfYZ + FZ^2 = 0. \quad (5)$$

From Eqs. (1) and (4), (X,Y,Z) can be derived in term of x, y, z, and θ as follows:

$$\begin{aligned} X &= (x - X_c)\cos\theta - (z - Z_c)\sin\theta \\ &= x\cos\theta - X_c\cos\theta + Z_c\sin\theta, \\ Y &= y - Y_c, \\ Z &= (x - X_c)\sin\theta + (z - Z_c)\cos\theta \\ &= x\sin\theta - X_c\sin\theta + Z_c\cos\theta. \end{aligned}$$

Substituting X, Y, and Z above into Eq. (5) and collecting together the terms according to the powers of x and y, we get

$$A'x^2 + B'xy + C'y^2 + D'x + E'y + F' = 0,$$

where

$$\begin{aligned} A' &= Af^2\cos^2\theta + Df\cos\theta\sin\theta + F\sin^2\theta, \\ B' &= Bf^2\cos\theta + Ef\sin\theta, \\ C' &= Cf^2, \\ D' &= -[2X_cA' + Y_cB' + Z_cM_1], \\ E' &= -[2Y_cC' + X_cB' + Z_cM_2], \\ F' &= X_c^2A' + X_cY_cB' + Y_c^2C' + X_cZ_cM_1 \\ &\quad + Y_cZ_cM_2 + Z_c^2M_3, \\ M_1 &= -2Af^2\cos\theta\sin\theta + Df(2\cos^2\theta - 1) \\ &\quad + 2F\sin\theta\cos\theta, \\ M_2 &= -Bf^2\sin\theta + Ef\cos\theta, \\ M_3 &= Af^2\sin^2\theta - Df\cos\theta\sin\theta + F\cos^2\theta. \end{aligned} \quad (6)$$

On the other hand, because the equation of a circle in the x-y plane of the OCS is $x^2 + y^2 = R^2$, relating the coefficients of this equation with those of the derived circle equation Eq. (6), we get

$$\begin{aligned} &A' = K, \quad B' = 0, \quad C' = K, \\ &D' = 0, \quad E' = 0, \quad F' = -KR^2 = -A'R^2, \end{aligned} \quad (7)$$

where K is a proportional factor. From the expressions of A' and C' in Eq. (6) and the observation, $A' = C'$, the tilt angle is derived as follows :

$$\begin{aligned} 1 &= \frac{A'}{C'} \\ &= \frac{A}{C}\cos^2\theta + \frac{D}{Cf}\cos\theta\sin\theta + \frac{F}{Cf^2}\sin^2\theta \\ &= a\cos^2\theta + b\cos\theta\sin\theta + c\sin^2\theta \end{aligned} \quad (8)$$

where

$$a = \frac{A}{C}, \quad b = \frac{D}{Cf}, \quad c = \frac{F}{Cf^2}.$$

Substituting $\sin^2\theta = 1 - \cos^2\theta$, $\cos^2\theta = \frac{\cos 2\theta + 1}{2}$, and $\cos\theta\sin\theta = \frac{\sin 2\theta}{2}$ into Eq. (8), we have

$$(1 - c) = (a - c)\frac{\cos 2\theta + 1}{2} + b\frac{\sin 2\theta}{2},$$

or equivalently,

$$d + e\cos 2\theta = b\sin 2\theta, \quad (9)$$

where

$$\begin{aligned} d &= 2(1 - c) - (a - c), \\ e &= -(a - c). \end{aligned}$$

Then, taking the squares on both sides of Eq. (9) and rearranging the terms according to the powers of $\cos 2\theta$ results in

$$a_1\cos^2 2\theta + a_2\cos 2\theta + a_3 = 0, \quad (10)$$

where

$$\begin{aligned} a_1 &= b^2 + e^2, \\ a_2 &= 2de, \\ a_3 &= d^2 - b^2. \end{aligned}$$

From Eq. (10) we get

$$\cos 2\theta = \frac{-a_2 \pm \sqrt{a_2^2 - 4a_1a_3}}{2a_1},$$

and so the desired solution is

$$\theta = \frac{1}{2}\cos^{-1}\left(\frac{-a_2 \pm \sqrt{a_2^2 - 4a_1a_3}}{2a_1}\right). \quad (11)$$

Next, the position parameters of the wheel center can be derived by the backprojection principle which is described below. As shown in Figure 4, after backprojecting the point P in the image into the CCS, we can get a line L which passes the lens center and P. The intersection point P′ of this line L and the horizontal plane, denoted by Π, whose y coordinate (the height of the wheel center) is known, is the corresponding space point of P which we want. Denote this point as P′.

The equation of the horizontal plane Π can be set as $y = h$. Assume that point P in the image plane has the CCS coordinate $(u_p, v_p, -f)$ where (u_p, v_p) is the position in the image and f is the focus length. In addition, the equation of line L is

$$\frac{x}{u_p} = \frac{y}{v_p} = \frac{z}{-f} = k. \quad (12)$$

Since point P′ is the intersection point of the plane Π and line L, by substituting $y = h$ into Eq. (12), the desired

CCS coordinates (x_p', y_p', z_p') of the wheel center of the lateral vehicle can be solved to be :

$$x_p' = u_p \cdot \frac{h}{v_p},$$
$$y_p' = h, \qquad (13)$$
$$z_p' = -f \cdot \frac{h}{v_p}.$$

3. Image Processing Techniques

As shown in Figure 3, the wheel shape of a vehicle in an image is an ellipse. Hence, ellipse detecting techniques must be used. In this study, the sobel operator is first applied to extract edge points. Then, the generalized Hough transform [7] is applied. Because the result might include ambiguous ellipses, an additional verification procedure is used to obtain a more precise candidate. There are four stages in the image processing works, which are shown as a flowchart in Figure 5. Stages 3 and 4, the edge verification algorithm, in Figure 5 will be expressed as a detailed algorithm later.

In the first stage, the sobel operator is used to obtain the edge points of the input image. The threshold value for the sobel operator is set as 300 by our experimental experiences.

In the second stage, a two-pass Hough transform procedure is applied. The inputs to the Hough transform are the coordinates (x_i, y_i) of detected edge points, and the parameter space is a four-dimensional counting space, i.e., a space of (x_0, y_0, a, b) in which the parameters come from the ellipse equation $\frac{(X - x_0)^2}{a^2} + \frac{(Y - y_0)^2}{b^2} = 1$, where (x_0, y_0) is the center of an ellipse and (a, b) are the minor and major diameters. The original input image is a 762×506 image. First, the image is reduced to 126×190 for finding the ellipse quickly. After the first-pass of Hough transform, a rough location of the center and two diameters are obtained. Next, a rectangular region in the original half-resolution (381×253) image obtained from the detected parameters is processed by the Hough transform again to get a more precise solution. This situation is shown in Figure 6.

In practical experimental situations, it is possible that the parameter set with the maximum cell counting value is not the exact solution. However, the more precise solution must be in neighborhood around one of the cells with larger cell counting values, so a verification procedure is applied in the third stage. The cells with counting values larger than 70% of the maximum counting value are checked in the following way. Let the ellipse curve inferred by each of the obtained parameter sets overlap the image of extracted edge points. The one with the maximum number of overlapping edge points is considered to be a candidate with a good parameter set. However, this edge verification process could not resolve the existence of ambiguous ellipses completely. By inspecting the experimental results, we see that the desired precise ellipse is the largest in shape of all candidates obtained in the third step. Hence, the ellipse with the maximum sum of the major and the minor diameter values is selected to be the detected ellipse of a wheel in this study. The detail of the verification algorithm is described in Algorithm 1.

Algorithm 1 : Verification for removing ambiguous ellipses obtained from Hough transform

Step 1. Find the cell with the maximum cell counting value (denoted as *MC*) after the Hough transform.

Step 2. Select all cells with their cell counting values > $0.7 \times MC$. Let these cells be denoted as C_i, i=1,2,... .

Step 3. For each cell C_i, calculate the equation of the corresponding ellipse using the corresponding parameters. Check the 60 points on the ellipse curve with 0, 6, 12, 18, ...254 degrees to see whether these points overlap an edge point in the edge-point image. Count the number of overlapping points, and denote it by ON_i.

Step 4. If there is only one maximum in all of the ON_i values, output the ellipse with the parameters of the cell corresponding to the maximum as the desired result and halt. Otherwise, continue.

Step 5. Let the maximum of the ON_i values be denoted as *MON*. For each cell C_j with the *MON* value, calculate the sum of the values of the major and minor diameters of the corresponding ellipse, and denote the result as DS_j. Find the cell C_{max} with the maximum DS_j and output the ellipse with the parameters of the cell C_{max} as the desired result and halt.

4. Experimental Results

4.1 Results of Image Processing

An example of the image processing result of ellipse detection is shown in this section. Figure 7 is the input image. After applying the sobel edge operator, the resulting edge-point image is shown in Figure 8. Then, the Hough transform was applied. The maximum cell counting value is 25, and there are 35 cells with their cell counting values larger than the threshold value $0.7 \times 25 = 17.5$. The parameters and the counting values of these cells are listed in Table 1. For each of the 35 cells, we calculated the overlapping edge point number. There are 4 cells in the results with the maximum number of overlapping edge points, which are listed in Table 2. Finally, the cell with the maximum sum of the major and the minor diameter values is selected as the desired result. In this example, cell 14 is accepted as the final precise solution. At last, the corresponding ellipse was drawn in

Figure 9 with black pixels as the result of wheel shape detection.

4.2 Experimental Results of Simulation

In the perspective projection model, the projection of a circle is an ellipse with rotation in most cases. However, it is assumed in this study that the projection of a wheel is an ellipse without rotation, i.e., an ellipse of the equation $\frac{(X-x_0)^2}{a^2}+\frac{(Y-y_0)^2}{b^2}=1$, for the reason of speeding up the Hough transform in detecting ellipse shapes because accordingly the dimensionality of the Hough counting space can be reduced by one. That is, we use an ellipse without rotation to approximate a real ellipse with rotation in a small angle in our experiments, so an error factor for the orientation parameter is introduced. A computer simulation process is designed in this study to test whether the error is in a tolerable range for real applications. First, a circle is projected onto the image plane, in which the center of the circle is located in a range with Z_c from 100 cm to 350 cm in intervals of 50cm, X_c from $-Z_c$ to 400 cm and rotation angle θ from 5 degrees to 75 degrees in intervals of 5 degrees. Second, a least square fit method is used to approximate the precise ellipse with an ellipse with no rotation. At last, the parameters of the equation of the approximate ellipse are substituted into Eqs. (8) through (11) derived in Section 2. The results of error analysis are shown in Table 3. It is seen that the average error of the rotation angle is smaller than 1°. Hence, the approximation of an ellipse with rotation by an ellipse without rotation is feasible in practice.

In the backprojection stage, the height of the wheel center should be known in advance. By measuring the heights of the wheel centers of a lot of cars of different models and manufacturers, we obtained the range of the height values to be from 27.5cm to 31.5cm. Because in the process of lateral vehicle location, the kind of the wheels on the vehicle are unknown in advance, we assume that the heights of the wheel centers of all cars are the same. In this way, an error factor for the translation parameter is introduced, so another computer simulation experiment was conducted to test whether the error is tolerable or not. First, the wheel center was projected onto the image plane by a set of the precise translation parameters. Then the backprojection process derived in Section 2 was applied under the assumption that the heights of the wheel centers of all cars are 29cm, which is the average value of the range of the wheel center heights from 27.5cm to 31.5cm. The results are shown in Table 4. The average error rate of the translation parameters are small than 5%, so the assumption of constant wheel center heights is considered feasible in practice.

4.3 Experimental results for real images

The proposed method was applied to two sets of images. In the first set, each image is independent. The results of image processing of the first set are shown in Figure 10. In the second set, three images of a sequence were used. The results of image processing of the second set are shown in Figure 11. The results of location of the two sets are listed in Table 5 and Table 6, respectively. In each of these tables, the column 'M' of each parameter is measured manually and was used as a reference to test the precision of the corresponding location result. The column 'm' of each parameter was obtained by the formula derived in Section 3. At last, the column 'e' of each table is the error measurement. For the translation parameters, i.e., for X and Z, the value of column 'e' specifies an error rate, which is the ratio of the difference between column 'M' and column 'm' to the value of 'M'. For the rotation parameter, the value of column 'e' denotes the difference between column 'M' and column 'm'. As shown in Table 5 and Table 6, the error rate values are less than 5%, so the proposed method is feasible for locating a lateral vehicle.

5. Conclusions and Future Works

A new approach to the detection of moving vehicle locations for driving assistance using single 2-D lateral vehicle images by 3-D computer vision techniques has been proposed. The rear wheel shape information in a lateral vehicle image is used to infer an analytical solution of the orientation angle and the relative position of the lateral vehicle respect to the driver's vehicle. The Hough transform is applied to detect the ellipse shape of the wheel in the image. To improve the accuracy of extracted ellipse shapes, an ellipse edge point verification algorithm has been developed. Both computer-simulated and real images were tested and good experimental results prove the effectiveness of the proposed approach. To extend the ability of the autonomous vehicle for driving assistance or vehicle guidance, it is interesting to estimate the motion of a lateral vehicle by a sequence of images when the time interval of two contiguous images is known. On the other hand, the combination of the front and rear wheel shape information to predicate the trajectory of a lateral vehicle, which is useful for vehicle avoidance, is also worth study.

References

[1] P. Y. Ku and W. H. Tsai, "Model-based guidance of autonomous land vehicle for indoor navigation," *Proc. of Workshop on Computer Vision, Graphics and Image Processing*, Taipei, Taiwan, R.O.C., pp.165-174, Aug, 1989.

[2] P. S. Lee, Y. E. Shen, and L. L. Wang, "Model-Based Location of Automated Guided Vehicles in the Navigation Sessions by 3D Computer Vision," *Journal of Robotic Systems*, Vol. 11, No. 3, pp.181-195, 1994

[3] N. M. Charkari, and H. Mori, "A New Approach for Real Time Moving Vehicle Detection," *Proceedings of the 1993 IEEE/RSJ Int. Conf. on Intelligent Robots and Systems*, Yokohama, Japan, pp. 273-278, 1993.

[4] K. Sasaki, N. Ishikawa, T. Otsuka, M. Nakajima, "3-D Image Location Surveillance System for the Automotive Rear-View," *Vehicle Navigation and Information Systems Conference Proceedings*, Yokohama, Japan, pp.27-32, 1994.

[5] Yamagchi, and Nakajima, "Development of an Observation System for the Automotive Rear View using a Fiber Grating Visual Sensor," *Sensor Technology*, Vol. 13, No. 4, 1993, pp. 18-22.

[6] R. Chapuis, A. Potelle, J. L. Brame, and F. Chausse, "Real-Time Vehicle Trajectory Supervision on the Highway," *International Journal of Robotics Research*, Vol. 14, No. 6, pp. 531-542, 1995.

[7] D. Pomerleau and T. Jochem, "Rapidly Adapting Machine Vision for Automated Vehicle Steering," *IEEE Expert*, Vol. 11, No. 2, pp.19-27, 1996.

[8] D. H. Ballard, "Generalizing the Hough Transform to detect arbitrary shapes," *Pattern Recognition*, Vol.13, No. 2, pp.111-122, 1981.

[9] R. M. Haralick and L. G. Shapiro, *Computer and Robot Vision, Volume 2*, Addison-Wesley, Reading, MA, U.S.A., 1993.

[10] R. C. Gonzalez and R. E. Woods, *Digital Image Processing*, Addison-Wesley, Reading, MA, U.S.A., 1992.

Table 1. Result of Hough transform.

Index	ON	y	x	a	b	cell counting value
0	59	99	327	17	24	25
1	58	103	327	18	28	25
2	59	103	328	18	27	25
3	59	102	327	17	26	22
4	59	102	327	18	27	22
5	59	103	327	17	27	22
6	46	104	327	18	29	22
7	47	107	327	18	31	22
8	58	99	325	15	23	21
9	59	100	325	15	24	21
10	60	100	327	17	25	21
11	58	102	328	18	28	21
12	39	99	328	19	31	20
13	59	102	325	15	26	20
14	60	102	327	17	27	20
15	42	102	329	19	28	20
16	43	106	327	19	31	20
17	59	98	327	17	23	19
18	59	101	325	15	25	19
19	59	101	326	17	26	19
20	60	101	327	17	25	19
21	49	104	325	16	28	19
22	59	104	328	18	26	19
23	60	104	330	16	26	19
24	40	106	326	19	30	19
25	38	106	326	20	31	19
26	59	101	327	18	26	18
27	45	101	328	18	29	18
28	59	102	326	17	27	18
29	58	103	325	16	27	18
30	53	103	327	19	28	18
31	40	104	326	19	28	18
32	44	106	327	18	30	18
33	59	106	329	18	24	18
34	59	107	330	15	23	18

Table 2. Result of edge verification.

Index	ON	y	x	a	b	cell counting value
10	60	100	327	17	25	21
14	60	102	327	17	27	20
20	60	101	327	17	25	19
23	60	104	330	16	26	19

Table 3. Simulation results of orientation angle computation.

θ(°)	X(cm)	Z(cm)	θ'(°)	Error(°)
5.0	-73.47	-304.26	5.04	0.04
15.0	-18.95	-315.66	15.37	0.37
25.0	36.15	-314.15	25.99	0.99
35.0	20.52	-290.82	36.19	1.19
45.0	-35.36	-318.19	45.73	0.73
55.0	20.43	-319.50	55.97	0.97
65.0	-36.15	-314.15	65.51	0.51
75.0	18.94	-315.66	75.58	0.58
85.0	73.47	-307.57	85.64	0.64

Table 4. Simulation results of backprojection of the wheel center.

height o wheel center (cm)	height of camera					
	67.5(cm)		68.5(cm)		69.5(cm)	
	X	Z	X	Z	X	Z
27.5	5.00%	5.00%	4.88%	4.88%	4.76%	4.76%
28.5	2.56%	2.56%	2.50%	2.50%	2.44%	2.44%
29.5	0.00%	0.00%	0.00%	0.00%	0.00%	0.00%
30.5	2.70%	2.70%	2.63%	2.63%	2.56%	2.56%
31.5	5.55%	5.55%	5.40%	5.40%	5.26%	5.26%

height o wheel center (cm)	height of camera					
	70.5(cm)		71.5(cm)		72.5(cm)	
	X	Z	X	Z	X	Z
27.5	4.65%	4.65%	4.54%	4.54%	4.44%	4.44%
28.5	2.38%	2.38%	2.32%	2.32%	2.27%	2.27%
29.5	0.00%	0.00%	0.00%	0.00%	0.00%	0.00%
30.5	2.50%	2.50%	2.44%	2.44%	2.38%	2.38%
31.5	5.12%	5.12%	5.00%	5.00%	4.87%	4.87%

Table 5. Result of location for image set 1.

	X(cm)			Z(cm)		
	M	m	e(%)	M	m	e(%)
Fig. 10(a	24.00	23.4	2.5%	-452.36	-474.78	4.96%
Fig. 10(b	49.5	51.67	4.38%	-449.28	-466.67	3.87%
Fig. 10(c	55.90	57.27	2.45%	:-470.6	-491.89	4.5%
Fig. 10(d	-56.50	-58.34	3.25%	-458.53	-451.24	1.59%

	θ(°)		
	M	m	e(°)
Fig. 10(a	-15.37°	-16.50°	1.13°
Fig. 10(b	-25.79°	-25.65°	-0.14°
Fig. 10(c	-39.44°	-39.74°	0.30°
Fig. 10(d	-28.40°	-28.81°	0.39°

Table 6. The result of location for image set 2.

	X(cm)			Z(cm)		
	M	m	e(%)	M	m	e(%)
Fig. 11(a	52.80	55.33	4.79%	-424.73	-423.26	0.35%
Fig. 11(b	19.00	19.34	1.80%	-451.60	-443.90	1.70%
Fig. 11(c	-30.8	-31.91	3.60%	-470.99	-451.24	4.19%

	θ(cm)		
	M	m	e(°)
Fig. 11(a	-36.91°	-37.19°	0.28°
Fig. 11(b	-36.91°	-35.74°	-1.17°
Fig. 11(c	-36.91°	-35.70°	-1.21°

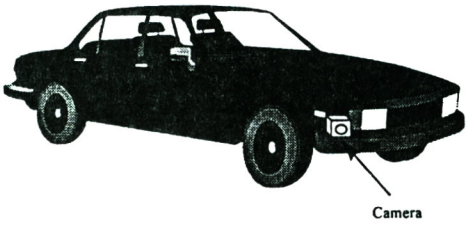

Figure 1. Illustration of a vehicle mounted with a camera for imaging lateral views.

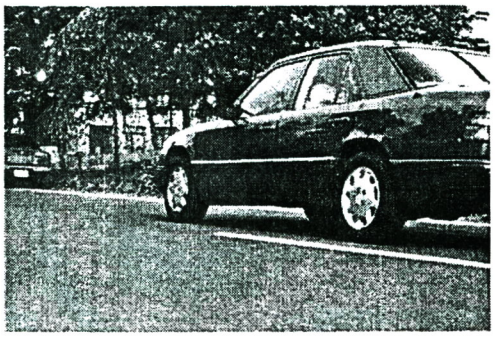

Figure 2. A typical lateral image through the camera view.

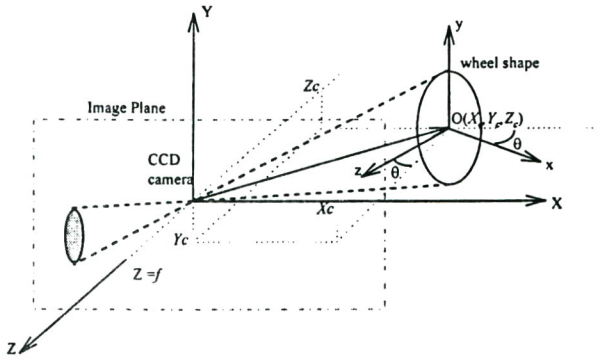

Figure 3. Geometrical description of coordinate systems for 3-D location estimation of a circular wheel shape.

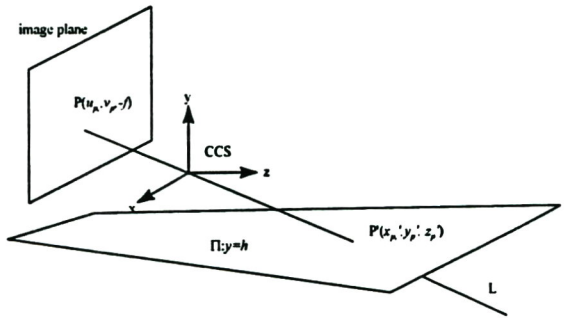

Figure 4. Illustration of the backprojection principle for finding the space point corresponding to an image pixel.

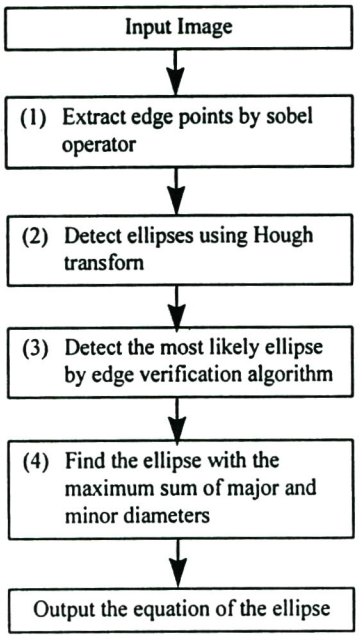

Figure 5. Flowchart of image processing processes.

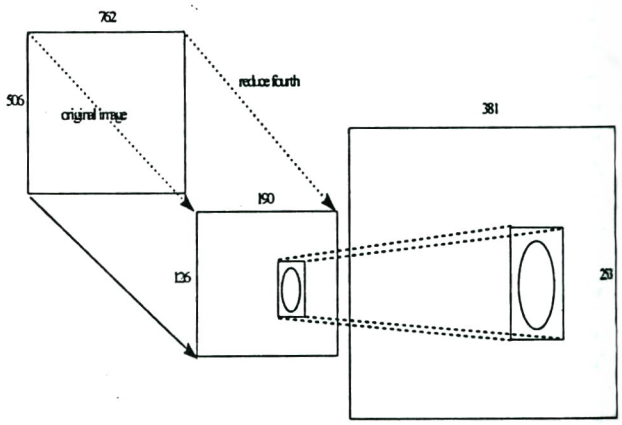

Figure 6. Illustration of 2-pass Hough transform.

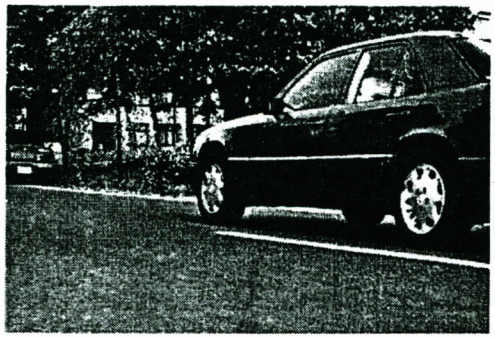

Figure 7. An example of input image.

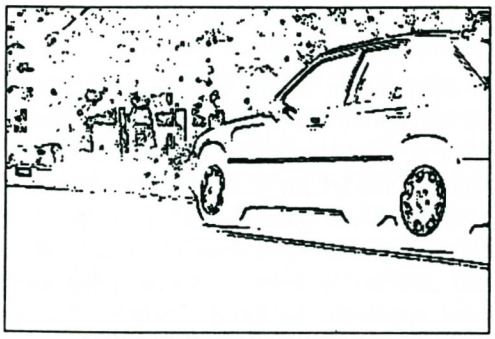

Figure 8. Result of edge detection.

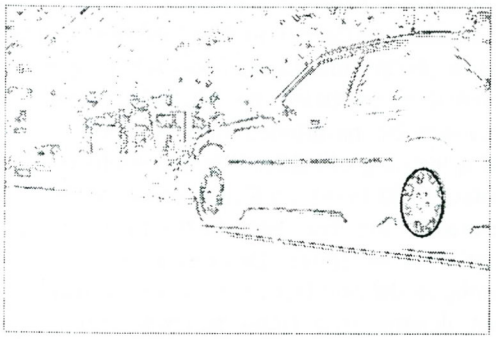

Figure 9. Result of ellipse detection.

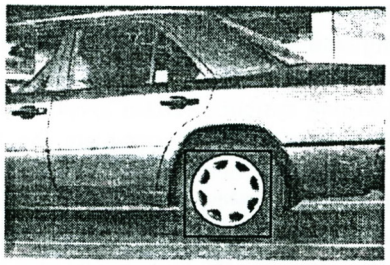

(a)

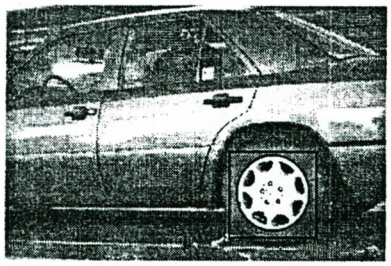

(b)

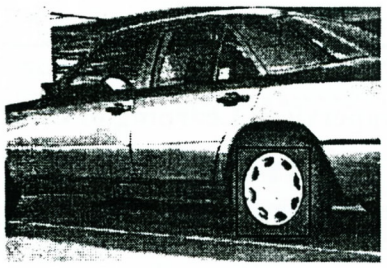

(c)

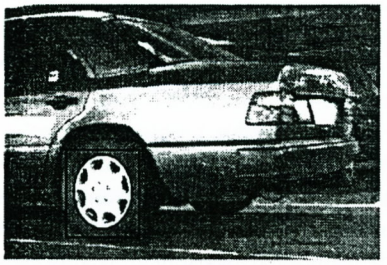

(d)

Figure 10. Results of image processing of image set 1.

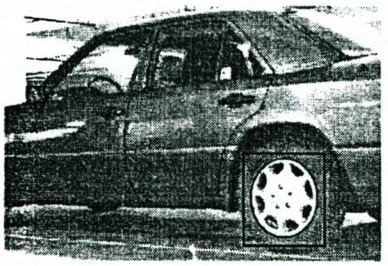

(a)

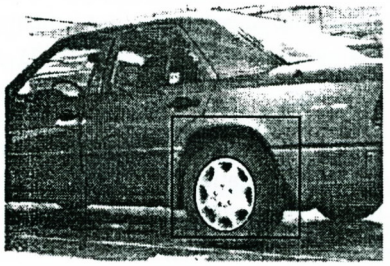

(b)

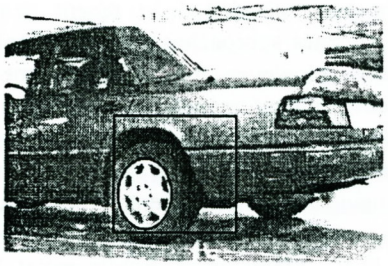

(c)

Figure 11. Results of image processing of image set 2.